

## ANALYSING TRANSIENT THERMOREFLECTANCE DATA USING NETWORK IDENTIFICATION BY DECONVOLUTION

Y. Ezzahri and A. Shakouri  
Department of Electrical Engineering, University of  
California Santa Cruz, Santa Cruz, California  
95064, USA

### ABSTRACT

Network Identification by Deconvolution (NID) method is applied to the analysis of the thermal transient pulsed laser heating. This is the excitation used in many optical experiments such as the Pump-Probe Transient Thermoreflectance experiment. NID method is based on linear RC network theory using Fourier's law of heat conduction. This approach is used to extract the thermal time constant spectrum of the sample after excitation by either a step or pulsed heat source at one surface. Furthermore, using network theory mathematical transformations, the details of the heat flux path through the sample can be analyzed. This is done by introducing the cumulative and differential structure functions. We show that the conventional NID method can be modified to analyze transient laser heating experiments. The advantage is that the thermal resistance of the top material layers and the major interface thermal resistances can be extracted without the need of assuming a specific multilayer structure. Some of the limitations due to the finite thermal penetration depth of the transient heat pulse will be discussed.

### INTRODUCTION

The most commonly used technique to measure the thermal conductivity of thin semiconductor films is the  $3\omega$  method developed by Cahill [1]. Reliable data obtained with this method are now used in many applications. A second interesting method is the Pump-Probe Transient Thermoreflectance technique (PPTTR), whose first utilization to study thermal transport experimentally was reported by Paddock and Eesley [2].

For nearly two decades, PPTTR technique has been an effective tool for studying heat transfer in thin films and low dimensional structures (multilayers and superlattices) [3]. In contrast to the  $3\omega$  method [1], PPTTR can distinguish between the thermal conductivity of thin films and their interface thermal resistance [3]. PPTTR is a time resolved technique

which extends the conventional thermoreflectivity technique [4] or flash technique [5], to very short time scales using femtosecond lasers and the optical sampling principle. The multiple advantages of this technique, being an entirely optical, non-contact and nondestructive method, with a high temporal resolution (on the order of the laser pulse duration  $<1\text{ps}$ ), and high spatial resolution (10nm in the cross-plane direction and  $<1\mu\text{m}$  in the in-plane direction), have conferred to it a particular place in the field of thermal properties metrology of thin metal and dielectric films. In this technique, an intense short laser pulse "pump" is used to heat the film, and a delayed weak (soft) short laser pulse "probe" is used to monitor the top free surface reflectivity change induced by the cooling of the thin film after absorption of the pump pulse. The pump and probe can come from the same primary laser source, a configuration called *homodyne PPTTR* [6], or they can be issued from two independent laser sources, a configuration called *heterodyne PPTTR* [7]. The heterodyne configuration allows having a long time delay between the pump and the probe that can go up to one period of the pump laser beam, which is for a  $76\text{MHz}$  Ti:sapphire source on the order of  $\sim 13\text{ns}$ . With the use of a pulse picker one can reach even longer time delays. Cumulative thermal effects could be important in certain PPTTR configurations in which the external modulation of the pump beam is used and it is on the same order of magnitude as the laser repetition rate [8, 9]. Here we focus on the inherent transient thermal response which can very well be modeled considering delta pulse heating with a laser.

Semiconductor and dielectric structures are usually covered by a thin metal film which acts as a thermal capacitor and temperature sensor [6]. The cross-plane thermal conductivity of the sample's top layer and the interface thermal resistance with the metal film are determined by comparing experimental cooling curves to theoretical simulations and optimization of free parameters to get the best fit [6]. In addition to the characterization of thermal properties of thin

films, PPTTR has also been proven a powerful tool for the characterization of acoustic properties of these films and other low dimensional structures [10, 11], a technique sometimes called picosecond ultrasonics.

In this paper we present an alternative method based on the RC network theory of linear passive elements to analyze the thermal decay of a PPTTR signal in which no cumulative effect is necessary to model the transient thermal response. This approach is called *Network Identification by Deconvolution* (NID). NID is a powerful technique proposed in the late 1980's by Székely and Van Bien [12]. This technique has been used to evaluate the thermal response of packaged semiconductor devices. These measurements can be used to separate different contributions to the total thermal resistance and capacitance of the sample under study. They are also used to identify structure defects and heat conduction anomalies. NID has introduced a new representation of the dynamical thermal behavior of semiconductor packages known as differential structure function or briefly *structure function* [12]. Using this quantity, the map of the heat current flow as a function of the cumulative thermal resistance in the sample can be obtained starting from the excited top free surface. In Székely's method, the temperature response is transformed to the time constant spectrum by deconvolution technique, and then, the time constant spectrum is transformed into two characteristic functions; the cumulative structure function and the differential structure function. These functions are defined as the variation of the cumulative thermal capacitance as a function of the cumulative thermal resistance along the heat flow path, and the first derivative of this function with respect to the cumulative thermal resistance, respectively [12-13]. By interpreting these functions, thermal resistances and capacitances of each part in the sample can be identified [13].

So far, NID method has been applied to various electronic and optoelectronic devices inside a package [12-14]. Recently, Fukutani et al [15] have successfully used the NID method for thermal characterization of Si/SiGe thin film microrefrigerators. All the results show that NID technique is a powerful method to identify thermal resistances in the heat flow path.

Still, most of the utilization of the NID method has been limited to the case of step function thermal transient measurements, with a recent interest in pulse thermal transients [16, 17]. In this paper, we apply this method to analyze the thermal transients of a structure after it is excited by a short laser pulse excitation. More precisely, we will consider the case of a delta function excitation applied to the top free surface of the sample. This is the usual case in a PPTTR experiment.

## NOMENCLATURE

- $\alpha_i$ : thermal diffusivity of layer  $i$  ( $m^2/s$ )
- $\beta_i$ : thermal conductivity of layer  $i$  ( $W/m/K$ )
- $(\rho c)_i$ : specific heat per unit volume of layer  $i$  ( $J/m^3/K$ ).
- $\delta$ : Dirac delta function.
- $\tau_i$ : time constant of layer  $i$  (s).

- $\Sigma$ : area of the spot illuminated by the pump laser pulse ( $m^2$ ).
- $\Pi$ : input power density ( $W/m^2$ ).
- $\theta_{in}$ : temperature at the input of the layer in Laplace domain.
- $\theta_{out}$ : temperature at the output of the layer in Laplace domain.
- $\phi_{in}$ : heat flux at the input of the layer in Laplace domain.
- $\phi_{out}$ : heat flux at the output of the layer in Laplace domain.
- $d_i$ : thickness of layer  $i$  (m).
- $p$ : Laplace variable.
- $r$ : radius of the spot area illuminated by the pump laser pulse (m).
- $H$ : Heaviside step function.
- $R$ : Reflection coefficient of the top Aluminum film surface at the wavelength of the laser.
- $R_{Th}$ : thermal resistance ( $K/W$ ).
- $C_{Th}$ : thermal capacitance ( $J/K$ ).
- $Q$ : pump laser pulse energy (J).
- $T$ : temperature (K).
- $Z$ : thermal impedance ( $K/W$ ).
- $R_K$ : interface thermal resistance at the metal layer/semiconductor layer interface ( $K.m^2/W$ ).
- $R_\Sigma$ : Cumulative thermal resistance ( $K/W$ ).
- $C_\Sigma$ : Cumulative thermal capacitance ( $J/K$ ).
- $K_\Sigma$ : Differential structure function ( $W^2/s/K^2$ ).

## THEORY

The theory of Network Identification by Deconvolution (NID) method applied to the case of a step function excitation, is very well established [13], and has been reviewed in many other papers [14-18, 21]. We will show below that a simple modification will allow us to generalize the NID method to analyze the case of a delta function excitation.

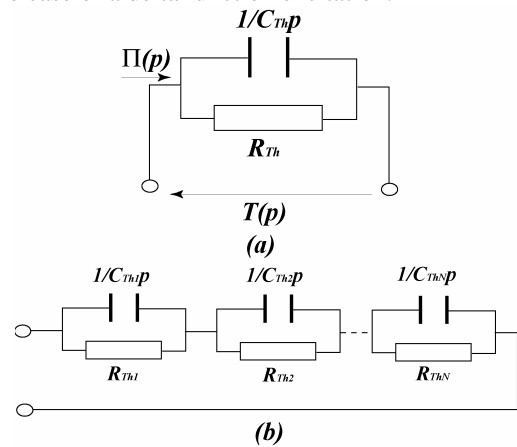


**Figure 1:** Schematic diagram of the RC one-port circuit of one layer (a) and the full structure (b).

If the diffusive regime is assumed to be valid in a material layer (the mean free path of phonons is much smaller than the thickness of the individual layer), then according to RC network theory, the thermal model of each layer could be described by a thermal resistance and a thermal capacitance.

Figure 1(a) shows a schematic diagram of the RC elements for one single layer. The thermal impedance of this layer is then calculated as the parallel connection of the thermal resistance  $R_{Th}$  and the thermal capacitive impedance  $1/C_{Th}p$ . This impedance could also be expressed using the time constant as well:

$$Z(p) = \frac{R_{Th} \times \frac{1}{C_{Th}p}}{R_{Th} + \frac{1}{C_{Th}p}} = \frac{R_{Th}}{1 + R_{Th}C_{Th}p} = \frac{R_{Th}}{1 + \tau p} \quad (1)$$

where  $p$  is called the complex frequency.  $\tau=R_{Th}C_{Th}$  is the time constant which is characteristic of the thermal behavior of the layer.

By applying a power function  $\Pi(p)$ , the temperature variation across the layer is given by the product of the thermal impedance and the power function in the frequency domain; this is the analogous of the well known Ohm's law in electricity.

$$T(p) = Z(p) \times \Pi(p) = \frac{R_{Th}}{1 + \tau p} \Pi(p) \quad (2)$$

The temperature variation is a function of the power function  $\Pi(p)$  used to excite the sample top free surface. Székely et al [12, 13, 16, 17], and other authors [14, 15], have emphasized the study of a step power excitation which is used in the electronic package characterization. In this case the excitation power is given by  $\Pi(t) = \Pi_0 \times H(t)$  where  $H(t)$  is the Heaviside step-unit function. The temperature variation in Laplace (complex frequency) domain is then given by:

$$T_H(p) = \Pi_0 \frac{R_{Th}}{p(1 + \tau p)} \quad (3)$$

On the other hand, for the case of a delta function excitation applied to the top free surface of the sample, which is the usual case in a PPTTR experiment, the excitation power is given by the Dirac  $\delta$  function  $\Pi(t) = \Pi_0 \times \delta(t)$ . The temperature variation in Laplace domain is then given by:

$$T_\delta(p) = \Pi_0 \frac{R_{Th}}{1 + \tau p} \quad (4)$$

Comparison of equations (3) and (4) allows us to write:

$$T_\delta(p) = p \times T_H(p) \quad (5)$$

In the time domain, equation (5) means that delta impulse response function is simply the derivative of the step-unit response function, or reversely the step-unit response function is the integral of the delta impulse response function. By just integrating the measured delta impulse response function, we can find the step-unit response function and then apply the powerful NID method to analyze the heat flow in the structure [12, 18].

#### TEMPERATURE VARIATION AT THE TOP FREE SURFACE OF THE STRUCTURE UNDER STUDY

To be able to validate the application of NID to the case of a delta-pulse function excitation, we have chosen a sample configuration typically used in a PPTTR experiment. Figure 2

shows a schematic diagram of the structure, which is assumed to be composed of a thin semiconductor Si/SiGe superlattice (SL) of different thicknesses and thermal conductivities deposited on top of a silicon substrate. In each case, the thin SL film is covered by a 30 nm thick Al film that will act as a thermal capacitor and temperature sensor, in which the temperature distribution is assumed to be uniform [6]. The thick silicon substrate is supposed to be semi-infinite.

Ti-sapphire pulsed laser sources are usually characterized by a laser frequency of 76MHz, which corresponds to a period of about 13.158ns. However, to study a wide time constant spectrum, we consider the frequency of the laser to be variable and the longest time delay could be up to 500ns, which corresponds to a frequency of 2MHz. Longer delays can be achieved experimentally using, for example, pulse-pickers. There is also a variety of picosecond and nanosecond pulsed laser sources which can reach microsecond or millisecond repetition periods. The time dependent temperature variation of the metal transducer is calculated using Thermal Quadrupoles Method (TQM) [19] and assuming one dimensional heat transport in the cross-plane direction. This approximation is justifiable considering the scale of the time delay (500ns) and a large size of the laser spot, which can easily go up to hundreds of  $\mu\text{m}$ . The dimension of the laser spot is taken to be larger than the thermal diffusion length of the sample under study. We consider a laser spot of radius  $r=10\mu\text{m}$ .

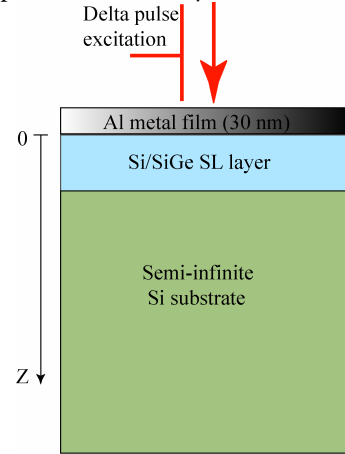


**Figure 2:** Schematic diagram of the structure under study deposited on a semi-infinite substrate.

Heat transport in the cross-plane direction of the structure is governed by the following set of equations:

$$(\rho C)_f d_f \frac{\partial T_f}{\partial t} = \beta_L^\perp \frac{\partial T_L}{\partial z} \Big|_{z=0} + \Pi(t, 0) \quad (6)$$

This equation describes the energy conservation at the interface between the metal transducer and the thin semiconductor layer (SC).  $(\rho C)_f$  and  $d_f$  are, respectively, the specific heat per unit volume and the thickness of the metal film.  $\beta_L^\perp$  is the cross-plane thermal conductivity of the SC layer, and  $\Pi$  represents the input flux which is given in the time domain by:

$$\Pi(t,0) = \frac{(1-R)Q}{\Sigma} \delta(t) \quad (7)$$

where  $R$  is the reflection coefficient of the metal film top free surface at the wavelength of the laser,  $Q$  is the laser pulse energy, and  $\Sigma$  is the illuminated area by the input flux at the metal film top free surface  $\Sigma = \pi r^2$ .

The interface metal transducer/semiconductor layer acts as a thermal barrier and thus, there is a jump in the temperature profile given by:

$$T_f - T_L = -\beta_L R_K \left. \frac{\partial T_L}{\partial z} \right|_{z=0} \quad (8)$$

where  $R_K$  is the thermal boundary resistance or Kapitza resistance at the interface.

Within the thin SC layer, and the silicon substrate, the temperature obeys the following equations:

$$\begin{cases} \frac{\partial^2 T_L}{\partial z^2} = \frac{1}{\alpha_L^+} \frac{\partial T_L}{\partial t} & \text{(Thin SC layer)} \\ \frac{\partial^2 T_S}{\partial z^2} = \frac{1}{\alpha_S^+} \frac{\partial T_S}{\partial t} & \text{(Substrate)} \end{cases} \quad (9)$$

where  $\alpha_L^+$  and  $\alpha_S^+$  are the cross-plane thermal diffusivities of the thin SC layer and the silicon substrate, respectively.

The interface between the thin SC layer and the silicon substrate is assumed to have no appreciable thermal resistance. To the above equations, we add the initial and boundary conditions given by:

$$\begin{cases} T_f(t=0) = T_L(t=0) = T_S(t=0) = 0 \\ T_S(z=\infty) = 0 \end{cases} \quad (10)$$

Solving this set of Eqs (6-10) becomes easier in Laplace domain using TQM. One can express the input temperature of the metal film  $\theta_f^{\text{in}}$  as a function of the input flux  $\phi_f^{\text{in}}$  in Laplace domain. The final relation is given by [21]:

$$\begin{cases} \theta_f^{\text{in}} = \frac{Z_{\text{sub}} A_L + B_L + Z_K (Z_{\text{sub}} C_L + D_L)}{\beta_f d_f \Sigma q_f^2 [Z_{\text{sub}} A_L + B_L + Z_K (Z_{\text{sub}} C_L + D_L)] + Z_{\text{sub}} C_L + D_L} \phi_f^{\text{in}} \\ \phi_f^{\text{in}} = (1-R)Q \end{cases} \quad (11)$$

where  $\beta_f$  is the thermal conductivity of the metal film,  $q_f^2 = \frac{p}{\alpha_f}$ ,

$p$  is Laplace variable and  $Z_K$  is the thermal resistance of the interface between the metal film and the thin SC layer  $Z_K = \frac{R_K}{\Sigma}$ . The heat transfer matrix coefficients of the SC

layer and the silicon substrate are given by:

$$\begin{cases} \begin{pmatrix} A_L & B_L \\ C_L & D_L \end{pmatrix} = \begin{pmatrix} \cosh[q_L d_L] & \frac{\sinh[q_L d_L]}{\beta_L^+ q_L \Sigma} \\ \beta_L^+ q_L \Sigma \times \sinh[q_L d_L] & \cosh[q_L d_L] \end{pmatrix} \\ \begin{pmatrix} A_S & B_S \\ C_S & D_S \end{pmatrix} = \begin{pmatrix} 1 & Z_{\text{sub}} = \frac{1}{\beta_S^+ q_S \Sigma} \\ 0 & 1 \end{pmatrix} \end{cases} \quad (12)$$

where  $q_{L,S} = \sqrt{\frac{p}{\alpha_{L,S}^+}}$ .

A numerical inverse Laplace transformation is finally used to

get the time domain temperature variation  $T_f^{\text{in}}(t)$ .  $T_f^{\text{in}}(t)$  represents the input signal to be analyzed by the NID method.

## RESULTS AND DISCUSSION

**Table 1:** Geometrical and thermal properties as well as the calculated thermal resistances and capacitances of the different layers in the structures under study.

layer	Si/SiGe SL	Si substrate
<b>Thickness <math>d_L</math> (nm)</b>	150	NA
	200	
	300	
<b>Thermal conductivity <math>\beta_L^+</math> (W/m/K)</b>	10	130
	15	
	20	
<b>Density <math>\rho_L</math> (kg/m<sup>3</sup>)</b>	2478.7	2329
<b>Specific heat <math>c_L</math> (J/kg/K)</b>	681	700
<b>Time constant <math>\tau_L</math> (ns)</b>	3.8 (SL <sub>1</sub> )	NA
	6.7 (SL <sub>2</sub> )	
	15.2 (SL <sub>3</sub> )	
	2.5 (SL <sub>4</sub> )	
	1.9 (SL <sub>5</sub> )	
<b>Calculated thermal resistance <math>R_{\text{Th}}^L</math> (K/W)</b>	47.7 (SL <sub>1</sub> )	NA
	63.7 (SL <sub>2</sub> )	
	95.5 (SL <sub>3</sub> )	
	31.8 (SL <sub>4</sub> )	
	23.9 (SL <sub>5</sub> )	
<b>Calculated thermal capacitance <math>C_{\text{Th}}^L \times 10^{-11}</math> (J/K)</b>	7.9 (SL <sub>1</sub> )	NA
	10.6 (SL <sub>2</sub> )	
	15.9 (SL <sub>3</sub> )	
	7.9 (SL <sub>4</sub> )	
	7.9 (SL <sub>5</sub> )	

In Fig 3, we show the calculated temperature decays  $T_f^{\text{in}}(t)$  of a SL structure, over a time range of 500ns with a 10ps time resolution after application of a delta power function to the top free surface of the structure. An amplitude of  $10^{-9}$ W is assumed. We have considered five different configurations of the structure with different thicknesses and thermal conductivities: SL<sub>1</sub> (150nm, 10W/m/K), SL<sub>2</sub> (200nm, 10W/m/K), SL<sub>3</sub> (300nm, 10W/m/K), SL<sub>4</sub> (150nm, 15W/m/K) and SL<sub>5</sub> (150nm, 20W/m/K). We have also assumed zero interface thermal resistance at the metal transducer/SC layer interface. Table 1, recapitulates the physical properties of the different layers in the structure.

The temperature decay reflects the transient heat flow as it penetrates through the whole structure (top metal film transducer + SC layer + Si substrate). In order to use the thermal decay to identify the thermal properties of the layers in the structure, we apply NID method using mathematical transformations.

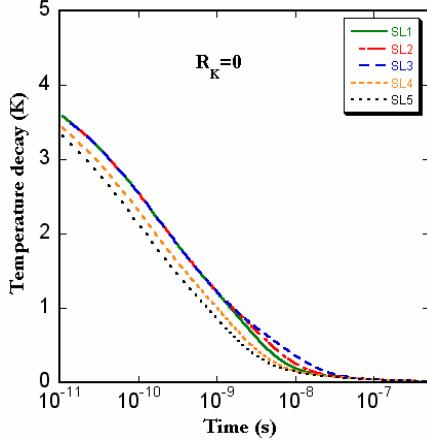


**Figure 3:** Calculated temperature decays over a 500ns time range with 10ps time resolution after application of a delta power function of amplitude  $10^{-9}W$  to the top free surface of the five structures under study.

The first step is the calculation of the time constant spectrum (TCS). This is obtained after integration of the delta impulse response function, transforming the result to the logarithmic time scale, differentiating it numerically and finally deconvolving it by a specific weight function [12, 18], using noise optimized Bayes iteration [13]. The result is reported in Figs 4(a) and 4(b).

As we can see in Figs 4(a) and 4(b), two main peaks are clearly distinguishable for each sample; these peaks represent the dominant time constants in the response function and they can be attributed to the SC layer and the portion of the silicon substrate that heat flow penetrates over the 500ns time range. In addition, the logarithmic representation in Fig 4(b) shows one more peak with small amplitude at early times. This secondary peak could be attributed to the temperature transient within the metal transducer.

The second step of the analysis consists of the evaluation of the cumulative structure functions and the differential structure function referred as *structure function* in brief [12]. We first plot the cumulative thermal capacitance  $C_{\Sigma}$  as a function of the cumulative thermal resistance  $R_{\Sigma}$  along the heat flow path and then we plot the derivative of this graph.  $C_{\Sigma}$  and  $R_{\Sigma}$  are defined respectively by the following equations:

$$\begin{cases} C_{\Sigma} = \int_0^x \rho c(y) \Sigma(y) dy \\ R_{\Sigma} = \int_0^x \frac{dy}{\beta(y) \Sigma(y)} \end{cases} \quad (13)$$

$x=0$  represents the top free surface of the structure where the excitation is applied. Evaluation of both graphs is based on the discretization of the time constant spectrum to get Foster representation of the RC network, then transforming Foster representation into Cauer-ladder representation which is suitable for physical interpretation [12-18]. The results are reported in Figs 5(a) and 5(b), respectively.

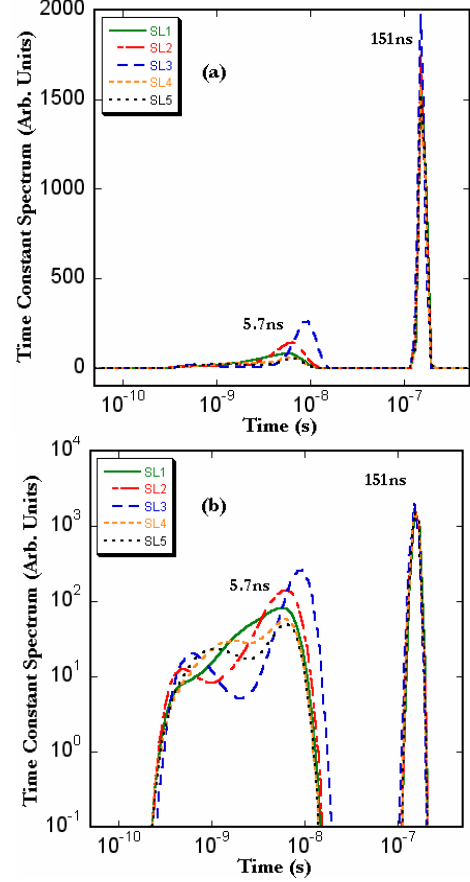


**Figure 4:** Time constant spectrums of the five structures over a time range of 500ns, obtained using NID method;  $SL_1$  (solid line),  $SL_2$  (solid-dashed line),  $SL_3$  (dashed line),  $SL_4$  (short dashed line) and  $SL_5$  (dotted line). All with 10ps time resolution and starting at 10ps. Log-lin representation (a) and log-log representation (b).

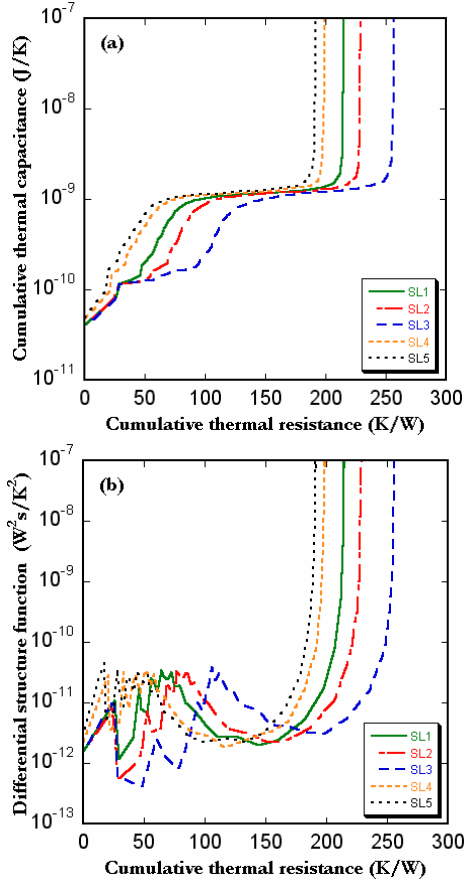
As we can see in these figures, each layer of the structure (dominant thermal resistance) is characterized by a slope in the cumulative structure function or a peak in the differential structure function, from which we can extract both the thermal resistance and capacitance of the SC layer. However we have found that the characteristic features shift by changing the time range of the thermal transient [18].

In Fig 6, we show the differential structure function of the sample 1 ( $SL_1$ ), over different measurement time ranges all starting at the same time 10ps and with the same 10ps time resolution, but truncated at different final times. The total thermal resistance increases by increasing the time range of the thermal transient due to heat diffusion within the silicon substrate. Based on the values of the total thermal resistances, we can easily verify the heat diffusion law

$$R_{Th}^{Tot} - R_{Th}^{SC} = \frac{L_s}{\beta_s \Sigma} = \frac{\sqrt{\alpha_s (t - \tau_{sc})}}{\beta_s \Sigma}$$

where  $L_s$ ,  $\beta_s$ , and  $\alpha_s$  are the penetration depth, thermal conductivity and thermal diffusivity

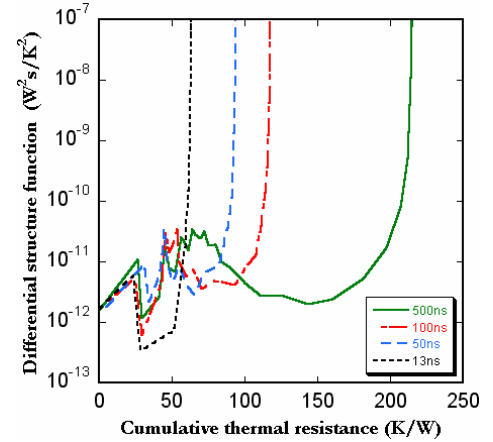
of the silicon substrate, respectively.  $\tau_{sc} = \frac{d_{sc}^2}{\alpha_{sc}}$ ,  $d_{sc}$ , and  $\alpha_{sc}$  are the calculated time constant, thickness and thermal diffusivity of the SC layer,  $t$  is total time range of the thermal transient, and  $\Sigma$  is the cross section area of the input flux.



**Figure 5:** Cumulative structure functions (a) and differential structure functions (b) of the five structures over a time range of 500ns; SL<sub>1</sub> (solid line), SL<sub>2</sub> (solid-dashed line), SL<sub>3</sub> (dashed line), SL<sub>4</sub> (short dashed line) and SL<sub>5</sub> (dotted line). All with 10ps time resolution and starting at 10ps.

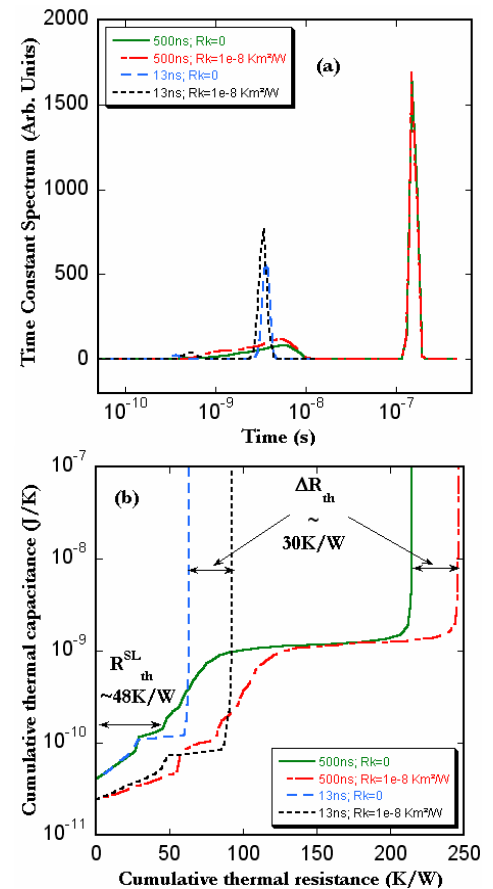
We can distinguish two peaks in the structure function that we attribute to the thermal transient of the metal transducer and the SC layer, respectively. We can see also that while the position of the first peak in the structure function is almost unchanged, the position of the second peak that is characteristic of the SC layer, shifts left to smaller times by decreasing the transient measurement time range. This is a consequence of the shift in the TCS [18].

The fact that the peaks of the TCS or the structure function shift by changing the time range, affects the value of the extracted thermal resistance and capacitance of the SC layer. That means that we have to find a time range interval that allows us to extract the accurate thermal properties of the SC layer using NID method. This analysis will be conducted later in the discussion.



**Figure 6:** Differential structure functions of the sample 1 under study (SL<sub>1</sub>) over different time ranges; 500ns (solid line), 100ns (solid-dashed line), 50ns (dashed line) and 13ns (short dashed line), all with 10ps time resolution and starting at 10ps.

#### EFFECT OF THE METAL/SC LAYER INTERFACE THERMAL RESISTANCE ON THE NID RESULTS



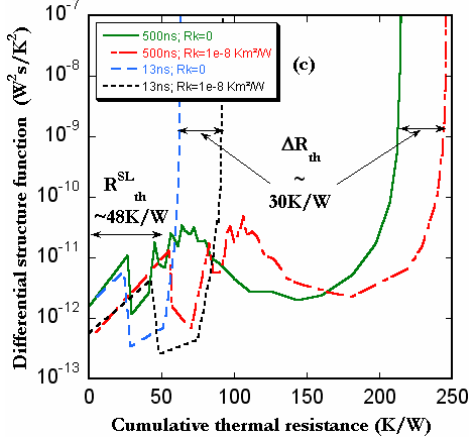


**Figure 7:** Time constant spectrums (a), cumulative structure functions (b) and differential structure functions (c) of the sample 1 (SL<sub>1</sub>) over two transient measurement time ranges 500ns (solid and solid-dashed lines) and 13ns (dashed and short dashed lines), all with 10ps time resolution, and starting at 10ps. Two different interface thermal resistances are considered  $R_K=0$  and  $R_K=10^{-8}\text{K}\cdot\text{m}^2/\text{W}$ .

Previously, we neglected the effect of the metal/SC layer interface thermal resistance  $R_K$ , and we have taken this resistance to be zero. In this paragraph, we will discuss this effect. Figure 7(a) shows the TCS of the sample 1 with Si/SiGe SL layer under study (SL<sub>1</sub>) over two different transient measurement time ranges, 500ns and 13ns, starting at the same time 10ps and with the same 10ps time resolution. For each time range, we consider two configurations; (i)  $R_K=0$ , and (ii)  $R_K=10^{-8}\text{K}\cdot\text{m}^2/\text{W}$ . We can see the slight shift to the right of the first peak in the TCS when  $R_K$  is different from zero. The shift is even clearer for a thermal transient over a short time range.

In Figs 7(b) and 7(c), we have reported the cumulative structure functions and the differential structure functions corresponding to the TCSs in Fig 7(a), respectively. Over both transient measurement time ranges, the effect of the interface thermal resistance is clear. The thermal resistance of the top layer is increased by an amount corresponding to  $R_K/\Sigma$  without affecting the extracted superlattice thermal resistance. This result proves the potential of using NID method to extract the interface thermal resistance between the metal transducer and the thin SC layer.

#### EFFECT OF NORMALIZATION ON THE NID RESULTS

So far in this discussion, we have shown the potential of using NID method to analyze thermal transients due to a delta function excitation using raw (calibrated) data of temperature variation  $\Delta T$  at the top free surface of the structure under study. In a PPTTR experiment, we measure the relative variation of the reflectivity of the surface  $\Delta R/R_0$ , which can be converted to a variation of temperature using a calibration process [4]. Often, in the analysis of the PPTTR signals, no calibration is used and the signals are normalized with respect to their initial values assuming a proportionality relation between  $\Delta R/R_0$  and

$\Delta T$ . We shall discuss in this paragraph the effect of normalization on the NID analysis.

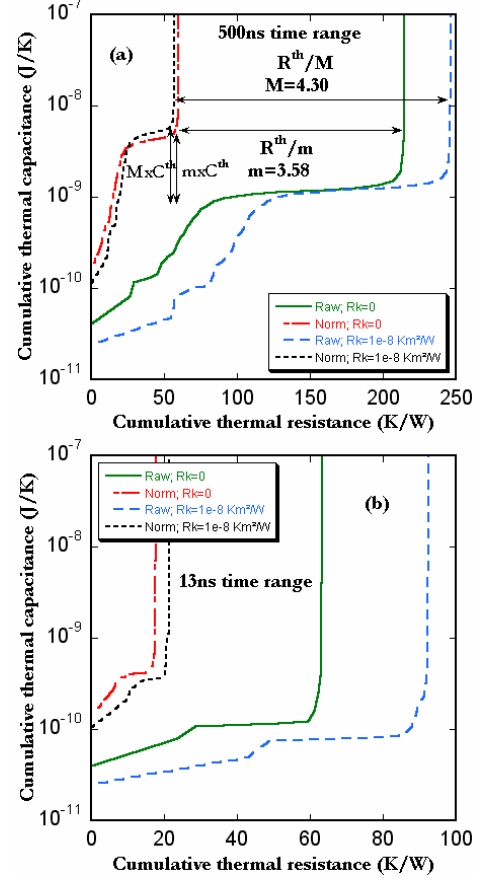


**Figure 8:** Cumulative structure functions of the SL<sub>1</sub> structure for raw (calibrated) and normalized delta function excitation signals over two transient measurement time ranges, 500ns (a) and 13ns (b), all with 10ps time resolution, and starting at 10ps. Two configuration are considered  $R_K=0$  (solid and solid-dashed lines) and  $R_K=10^{-8}\text{K}\cdot\text{m}^2/\text{W}$  (dashed and short dashed lines).

We show in Figs 8(a) and 8(b) the cumulative structure functions of the calibrated and normalized delta function excitation signals over two different time ranges, 500ns (a) and 13ns (b) starting at the same time 10ps and with the same 10ps time resolution. Two configurations are considered in each case, (i)  $R_K=0$  and (ii)  $R_K=10^{-8}\text{K}\cdot\text{m}^2/\text{W}$ . As can be seen in these figures, when normalized signals are used, the effect on the NID results is the introduction of a simple scaling factor  $m$ , where  $m$  is the amplitude of the signal at the initial time of the thermal transient. In terms of cumulative thermal resistances, cumulative thermal capacitances and structure functions, the results of NID are scaled according to the three relations:

$$R_{\text{Th}}^i(\text{Nor}) = R_{\text{Th}}^i(\text{Calibrated}) / m, \quad C_{\text{Th}}^i(\text{Nor}) = m C_{\text{Th}}^i(\text{Calibrated}) \quad \text{and} \\ K_{\text{Th}}^i(\text{Nor}) = m^2 K_{\text{Th}}^i(\text{Calibrated}).$$

Also we can see that because of the scaling effect introduced by the normalization, the difference of the total thermal resistance between the cases  $R_K=0$  and  $R_K \neq 0$  is also reduced. However it is possible to

extract the value of  $R_K$  using the relation  $R_K/\Sigma = MR_{Th}^{Tot} (Nor, R_K \neq 0) - mR_{Th}^{Tot} (Nor, R_K = 0)$ , where  $m$  and  $M$  are the amplitudes of the signal at the initial time of the thermal transient in the case  $R_K=0$  and  $R_K \neq 0$ , respectively.

**NEEDED TIME RANGE IN A PPTTR EXPERIMENT TO EXTRACT THE THERMAL PROPERTIES OF THE THIN SC FILM USING NID METHOD**

In the previous discussion of the NID method applied to the case of a semi-infinite substrate, which is realistic during the time delay in a PPTTR experiment, we have shown that the characteristic peak of the SC layer in the structure function varies by changing the time range of the thermal transient measurement. There is a need to find a time range interval within which the position of the peak will be the closest to the real value, and will allow determination of both the thermal resistance and capacitance of the SC layer, from which the thermal conductivity and specific heat per unit volume of this layer can be extracted. To determine this time interval, we have considered a Si/SiGe SL layer deposited on a semi-infinite silicon substrate and covered by a 30nm thin Al film with  $R_K=0$ . The thickness and thermal conductivity of the SL layer are varied to create three different configurations, which are (150nm, 10W/m/K), (150nm, 15W/m/K), and (100nm, 15W/m/K).

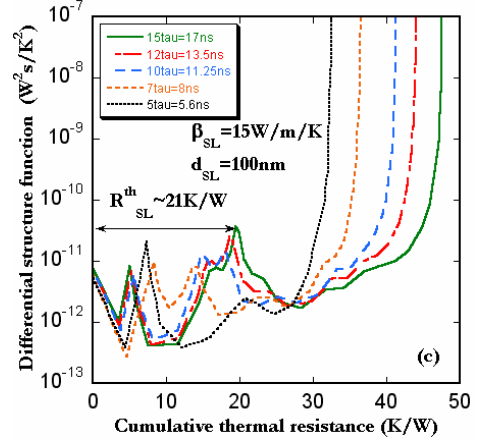
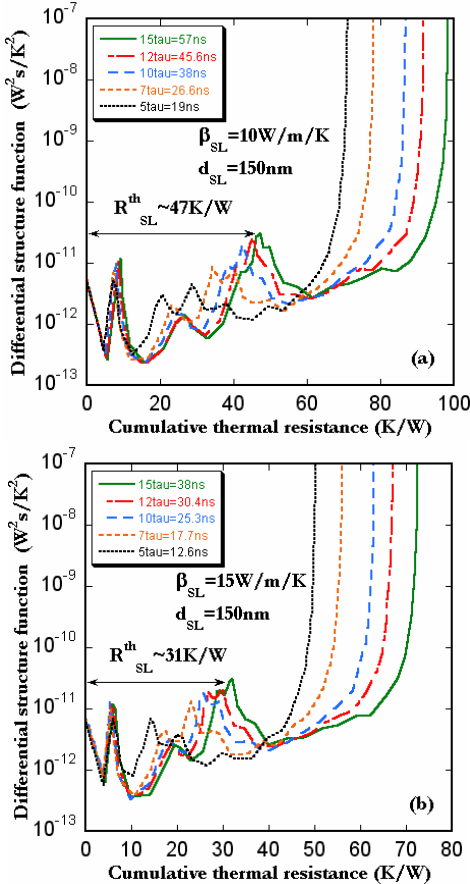


**Figure 9:** Differential structure functions of the superlattice sample with  $R_K=0$  for a delta function excitation over different time ranges,  $15\tau_{SC}$  (solid line),  $12\tau_{SC}$  (solid-dashed line),  $10\tau_{SC}$  (dashed line),  $7\tau_{SC}$  (short dashed line) and  $5\tau_{SC}$  (dotted line), all with 1ps time resolution, and starting at 1ps. (a) 150nm thick and 10W/m/K thermal conductivity SL, (b) 150nm thick and 15W/m/K thermal conductivity SL and (c) 100nm thick and 15W/m/K thermal conductivity SL.

The differential structure functions corresponding to a delta function excitation for the three different configurations of the structure under study are shown in Figs 9(a-c) over five different time ranges of the thermal transient  $15\tau_{SC}$ ,  $12\tau_{SC}$ ,  $10\tau_{SC}$ ,  $7\tau_{SC}$ , and  $5\tau_{SC}$  where  $\tau_{SC}$  represents the calculated time constant of the SC layer. For the three examples, the characteristic peak of the SC layer varies by changing the time range. We have found that a time range between  $10\tau_{SC}$  and  $15\tau_{SC}$  will allow determination of both the thermal resistance and capacitance of the SC layer with an error on the thermal resistance 2-3% for  $15\tau_{SC}$  and up to 20% for  $10\tau_{SC}$ . This error increases by decreasing the time range. We should note here that even though the input signals to the NID method are calculated analytically for each structure, the error on extracting thermal resistances and capacitances come from the different steps in the NID program parameter identification. Two key factors are the deconvolution and the number of RC ports used for the discretization of the time constant spectrum.

**CAN WE EXTRACT SIMULTANEOUSLY THE THERMAL CONDUCTIVITY OF THE SC FILM AND THE METAL/SC FILM INTERFACE THERMAL RESISTANCE FROM A SINGLE PPTTR EXPERIMENTAL SIGNAL USING NID METHOD?**

In order to answer this question and based on all previous discussions, we consider a real situation of the PPTTR experiment using a time delay of 13158ps with a 1ps time resolution, which is the state of the art of the heterodyne configuration without changing the frequency of the Ti: sapphire pulsed laser sources [7]. This time delay is taken to be the time range of the transient thermal decay due to a delta excitation of the top free surface of the structure under study.



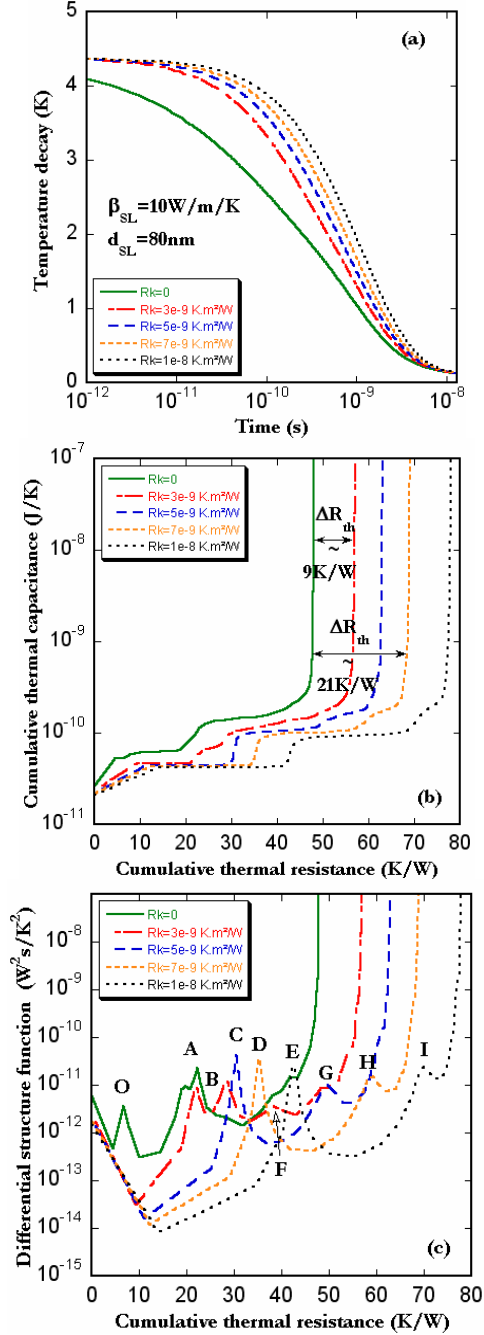


**Figure 10:** (a) Calculated temperature decays at the top free surface of the structure with an 80nm thick Si/SiGe SL layer deposited on a semi-infinite silicon substrate and covered by a 30nm thick Al film, with  $R_K=0$  (solid line),  $R_K=3 \times 10^{-9} \text{ K.m}^2/\text{W}$  (solid-dashed line),  $R_K=5 \times 10^{-9} \text{ K.m}^2/\text{W}$  (dashed line),  $R_K=7 \times 10^{-9} \text{ K.m}^2/\text{W}$  (short dashed line) and  $R_K=1 \times 10^{-8} \text{ K.m}^2/\text{W}$  (dotted line), after excitation by a delta laser pulse with an energy  $10^{-9} \text{ J}$  over a time range of 13ns with 1ps time resolution and starting at 1ps. Cumulative structure functions (b) and differential structure functions (c) corresponding to the temperature decays in (a).

According to the conclusion of the last section regarding the time range of the thermal transient, we assume the sample to be an 80nm Si/SiGe SL layer deposited on a semi-infinite silicon substrate and covered by a 30nm thick Al film. The thickness of the structure is small enough to satisfy the relation  $t=13158\text{ps} \approx 12\tau_{SC}$ . Five different values of the metal/SC layer interface thermal resistance are considered; (i)  $R_K=0$ , (ii)  $R_K=3 \times 10^{-9} \text{ K.m}^2/\text{W}$ , (iii)  $R_K=5 \times 10^{-9} \text{ K.m}^2/\text{W}$ , (iv)  $R_K=7 \times 10^{-9} \text{ K.m}^2/\text{W}$  and (v)  $R_K=1 \times 10^{-8} \text{ K.m}^2/\text{W}$ . As we have mentioned before, this is a typical PPTTR experiment.

Figure 10(a) illustrates the calculated temperature decays  $\Delta T$  at the top free surface of the structure after excitation of this surface by a delta laser pulse of energy  $10^{-9} \text{ J}$ . Increasing  $R_K$  not only raises the amplitude of  $\Delta T$ , but changes the temperature decay behavior over the first 10ns after where the curves start to overlap.

The cumulative structure functions and the differential structure functions corresponding to these five different configurations are reported in Figs 10(b) and 10(c), respectively. The effect of increasing  $R_K$  is clearly demonstrated in these figures where we can see the apparition of a new slope in the cumulative structure function or a new peak in the differential structure function which corresponds to an interface thermal resistance  $R_K \neq 0$ . The peaks A, F, G, H and I correspond to the SC layer. The extracted thermal resistance of the SC layer at the peak A is  $R_{Th}^{SC} \approx 22.3 \text{ K/W}$  and the corresponding thermal capacitance after subtraction of the initial value and the thermal capacitance of the 30nm thick Al film ( $\sim 2.3 \times 10^{-11} \text{ J/K}$ ) is  $C_{Th}^{SC} \approx 5 \times 10^{-11} \text{ J/K}$ . These values are in very good agreement with the theoretical values ( $25.5 \text{ K/W}$ ,  $4.24 \times 10^{-11} \text{ J/K}$ ). On the other hand, the peaks B, C, D and E are the characteristic peaks of  $R_K=3 \times 10^{-9} \text{ K.m}^2/\text{W}$ ,  $R_K=5 \times 10^{-9} \text{ K.m}^2/\text{W}$ ,  $R_K=7 \times 10^{-9} \text{ K.m}^2/\text{W}$  and  $R_K=1 \times 10^{-8} \text{ K.m}^2/\text{W}$ , respectively. The values at these peaks may include also the effect of the thermal transient of the metal transducer. The first peak O in the case  $R_K=0$ , is attributed to this thermal transient alone. We can see also that in all cases  $R_K \neq 0$ , the total thermal resistances are increased exactly by the amount equal to  $R_K/\Sigma$ .

These results show clearly the potential of application of NID method to extract both the thermal resistance of the SC layer and the metal/SC layer interface thermal resistance from a single PPTTR measurement in which no cumulative effect is needed to model the thermal transient [18]. We should note however, that while the error on the extracted thermal resistance of the SC layer is  $<12\%$  in the case  $R_K=0$ , this error increases in the case  $R_K \neq 0$ . On the other hand, the interface thermal resistance variation  $\Delta R_K$  can be easily determined by comparing the total thermal resistances values from the cumulative or differential structure functions. Generally, a comparison with a reference structure for which we know either the interface thermal resistance or the thermal conductivity will allow determination of the second parameter more accurately.

## CONCLUSION

We have discussed in this paper the possible application of NID method to the extraction of the thermal properties of a thin semiconductor layer deposited on a semi-infinite substrate, based on a PPTTR experiment in which the excitation can be modeled by a delta function and the cumulative effect can be neglected. We have discussed many configurations of the structure under study. One limitation of the method in the case of a semi-infinite substrate is the choice of the time range interval for the thermal transient. A time range between 10-15 times larger than the thin semiconductor layer thermal response time is needed to extract both the thermal resistance and capacitance of the thin layer with an error less than 20%.

We have demonstrated that within this time interval, the NID method can be of great interest to extract both the thermal conductivity of the thin semiconductor layer as well as the metal transducer/semiconductor layer interface thermal resistance from a single PPTTR signal. A comparison with a reference structure for which we know one of the parameters will allow determination of the second parameter even more accurately. The beauty of NID method is that it does not assume any given structure a priori (number of layers or interfaces). Peaks in the differential structure function show the different thermal resistances that can be separated. If layers are very thin, their thermal resistances will be combined and we can only extract the average property of the layers.

## ACKNOWLEDGMENTS

This work is supported by the Interconnect Focus Center, one of the five research centers funded under the Focus Center Research Program, a DARPA and Semiconductor Research Corporation program, as well as by AFOSR MURI grant number FA9550-08-1-0340.

## REFERENCES

- [1] Cahill. D. G, 1990, "Thermal conductivity measurement from 30 to 750 K: the  $3\omega$  method" Rev. Sci. Instrum, vol. **61**, pp. 802-808.
- [2] Paddock. C. A, and Eesley G. L, 1986, "Transient thermoreflectance from thin metal films", J. Appl. Phys, vol. **60**, pp. 285-290.
- [3] Cahill. D. G, Ford. W. K, Goodson. K. E, Mahan. G. D, Majumdar. A, Maris. H. J, Merlin. R, and Phillpot. S. R, 2003, "Nanoscale thermal transport", J. Appl. Phys, vol. **93**, pp. 793-818.
- [4] Dilhaire. S, Grauby. S, and Claeys. W, 2004, "Calibration procedure for temperature measurements by thermoreflectance under high magnification conditions", Appl. Phys. Lett, vol. **84**, pp. 822-824.
- [5] Parker. W. J, Jenkins. R. J, Butler. C. P, and Abbot. G. L, 1961, "Flash Method of Determining Thermal Diffusivity, Heat Capacity, and Thermal Conductivity", J. Appl. Phys, vol. **32**, pp. 1679-1684.
- [6] Ezzahri. Y, Grauby. S, Dilhaire. S, Rampnoux. J. M, and Claeys. W, 2007, "Cross-plan Si/SiGe superlattice acoustic

and thermal properties measurement by picosecond ultrasonics", J. Appl. Phys, vol. **101**, pp. 013705-013711.

- [7] Dilhaire. S, Claeys. W, Rampnoux. J. M, and Rossignol. C, 2007, "Optical Heterodyne Sampling Device", Patent, WO/2007/045773.
- [8] Cahill. D. G, 2004, "Analysis of heat flow in layered structures for time domain thermoreflectance" Rev. Sci. Instrum, vol. **75**, pp. 5119-5122.
- [9] Schmidt. A. J, Chen. X, and Chen. G, 2008, "Pulse accumulation, radial heat conduction and anisotropic thermal conductivity in pump probe transient thermoreflectance," Rev. Sci. Instrum, vol. **79**, pp. 114902-114910.
- [10] Rossignol. C, Perrin. B, Bonello. B, Djemia. P, Moch. P, and Hurdequint. H, 2004, "Elastic properties of ultrathin permalloy/alumina multilayer films using picosecond ultrasonics and Brillouin light scattering", Phys. Rev. B, vol. **70**, pp. 094102-094113.
- [11] Ezzahri. Y, Grauby. S, Rampnoux. J. M, Michel. H, Pernot. G, Claeys. W, Dilhaire. S, Rossignol. C, Zeng. G, and Shakouri. A, 2007, "Coherent phonons in Si/SiGe superlattices", Phys. Rev. B, vol. **75**, pp. 195309-195319.
- [12] Székely. V and Bien. T. V, 1988, "Fine structure of heat flow path in semiconductor devices: A measurement and identification method", Solid-State Electronics, vol. **31**, pp. 1363-1368.
- [13] Székely. V, 2002, "Enhancing reliability with thermal transient testing", Microelectronics Reliability, vol. **42**, pp. 629-640.
- [14] Ezzahri. Y, Singh. R, Fukutani. K, Bian. Z, Zeng. G, Zide. J. M, Gossard. A. C, Bowers. J. E, and Shakouri. A, 2007, "Transient thermal characterization of ErAs/In<sub>0.53</sub>Ga<sub>0.47</sub>As thermoelectric module", Proceeding of the InterPACK 2007, Vancouver, British Columbia, Canada, July 8-12.
- [15] Fukutani. K, Singh. R, and Shakouri. A, 2006, "Thermal transient characterization of packaged thin film microcoolers", Proceeding of the International Workshop on Thermal Investigations of ICs and Systems (THERMINICS), pp. 157-162, Nice, Côte d'Azur, France, September 27-29.
- [16] Szabo. P, Rencz. M, Farkas. G, and Poppe. A, 2006, "Short time die attach characterization of Leds for in-line testing application", Proceeding of the 8<sup>th</sup> EPTC conference, pp. 360-366, Singapore, Dec 6-8.
- [17] Székely. V, 2008, "Evaluation of short pulse thermal transient measurements", Proceeding of the International Workshop on Thermal Investigations of ICs and Systems (THERMINICS), pp. 20-25, Rome, Italy, Sept 24-26.
- [18] Ezzahri. Y and Shakouri A, "Application of Network Identification by Deconvolution method to the thermal analysis of the Pump Probe Transient Thermoreflectance signal", Accepted for Publication in Review of Scientific Instruments.
- [19] Maillet. D, André. S, Batsale. J. C, Degiovanni. A, and Moyne. C, 2000, "THERMAL QUADRUPOLES: Solving the Heat Equation through Integral Transforms", John Wiley & Sons.